The Cryosphere
Open Access
Discussions

Tracing glacial disintegration from the LIA to the present using a LIDAR-based hi-res glacier inventory

A. Fischer[1], B. Seiser[1], M. Stocker-Waldhuber[1,2], C. Mitterer[1], and
J. Abermann[3,*]

[1]Institute for Interdisciplinary Mountain Research, Austrian Academy of Sciences,
Technikerstrasse 21a, 6020 Innsbruck, Austria
[2]Institut für Geowissenschaften und Geographie, Physische Geographie,
Martin-Luther-Universität Halle-Wittenberg, Von-Seckendorff-Platz 4, 06120 Halle, Germany
[3]Commission for Geophysical Research, Austrian Academy of Sciences, Innsbruck, Austria
[*]now at: Asiaq – Greenland Survey, 3900 Nuuk, Greenland

Correspondence to: A. Fischer (andrea.fischer@oeaw.ac.at)

Discussion Paper | Discussion Paper | Discussion Paper | Discussion Paper

Title Page

Abstract	Introduction
Conclusions	References
Tables	Figures

|◄ | ►|
◄ | ►
Back | Close

Full Screen / Esc

Printer-friendly Version

Interactive Discussion

Abstract

Glacier inventories provide the basis for further studies on mass balance and volume change, relevant for local hydrological issues as well as for global calculation of sea level rise. In this study, a new Austrian glacier inventory updating data from 1969 (GI I) and 1998 (GI II) has been compiled, based on high resolution LiDAR DEMs and orthophotos dating from 2004 to 2011 (GI III). To expand the time series of digital glacier inventories in the past, the glacier inventory of the Little Ice Age maximum state (LIA) has been digitalized based on the LiDAR DEM. The resulting glacier area for GI III of $415.11 \pm 11.18\,\text{km}^2$ is 44 % of the LIA area. The area losses show high regional variability, ranging from 11 % annual relative loss to less than 1 % for the latest period. The glacier sizes reduced from LIA to the latest period, so that in GI III 47 % of the glaciers' areas are smaller than $0.1\,\text{km}^2$.

1 Introduction

The history of growth and decay of mountain glaciers affects society in the form of global changes in sea level and in the regional hydrological system as well as through glacier-related natural disasters. Apart from these direct impacts, the study of past glacier changes reveals information on palaeoglaciology and, together with other proxy data, palaeoclimatology and thus helps to compare current with previous climatic changes and their respective effects.

Estimating the current and future contribution of glacier mass balance to sea level rise needs accurate information on the area and elevation of the world's glacier cover. In recent years the information available on global glacier cover has increased rapidly, with global glacier inventories compiled for the IPCC Report 2013 (Vaughan et al., 2013) complementing the world glacier inventories (WGMS, 2012) and the GLIMS initiative (Kargel et al., 2014). These global inventories serve as a basis for modelling current and future global changes in ice mass (e.g. Gardner et al., 2013; Marzeion et al.,

2012; Radić and Hock, 2011). Based on the glacier inventories, ice volume has been modelled with different methods as a basis for future sea level scenarios (Huss and Farinotti, 2012; Linsbauer et al., 2012; Radić and Hock, 2010). On a regional scale, these glacier inventory data are used for calculating future scenarios of current local

5 and regional hydrology and mass balance (Huss, 2012). All these research is based on the most accurate mapping of glacier area and elevation at a particular point in time.

For large-scale derivation of glacier surfaces, satellite remote sensing methods are most frequently applied (Paul et al., 2010, 2011b, 2013). For direct monitoring of glacial recession over time, and the linkage of the loss of volume and area to local climatic and

10 ice dynamical changes, time series of glacier inventories are needed. Time series of remote sensing data naturally are limited by the availability of first satellite data (e.g. Rott, 1977), so that time series of glacier inventories have been limited to a length of several decades (Bolch et al., 2010). Longer time series (Nuth et al., 2013; Paul et al., 2011a; Andreassen et al., 2008) can only be compiled from additional data with varying

15 error characteristics (e.g. Haggren et al., 2007) and temporally and regionally varying availability of older data, limiting the availability of global sets of historical data. Apart from the inventories mentioned above, further extra-European regional time series of glacier inventories are available, for instance, for the Cordillera Blanca in Peru (Lopez-Moreno et al., 2014).

20 Glaciological data in the Alps are among the longest and densest time series. Apart from the Randolph glacier inventory data (Ahrendt et al., 2012) and a pan-Alpine satellite-derived glacier inventory (Paul et al., 2004, 2011b), several national or regional glacier inventories are available. For Italy, only regional data are available, for example, for South Tyrol (Knoll and Kerschner, 2010) and the Aosta region (Diolaiuti et al.,

25 2012). For the five German glaciers, time series of glacier areas have been compiled by Hagg et al. (2012). For the French Alps, glacier inventories have been compiled for 4 dates between 1967/1971 and 2006/2009 by Gardent et al. (2014). For Switzerland, several glacier inventories have been compiled from different sources. For the year 2000, a glacier inventory has been compiled from remote sensing data (Kääb et al.,

2002), for 1970 from aerial photography (Müller et al., 1976) and for 1850 the glacier inventory was reconstructed by Maisch et al. (1999). Elevation changes have been calculated between 1985 and 1999 for about 1050 glaciers (Paul and Haeberli, 2008) and recently by Fischer et al. (2014).

For the Austrian Alps, glacier inventories so far have been compiled for 1969 (Patzelt, 1980; GI I) and 1998 (Lambrecht and Kuhn, 2007; GI II) on the basis of orthophoto maps. Groß (1987) estimated glacier area changes between 1850, 1920 and 1969, mapping the extent of the Little Ice Age (LIA) and 1920 moraines from the orthophotos of the glacier inventory of 1969. As the Austrian federal authorities made LiDAR data available for the major part of Austria after years of very negative mass balances after 2000, these data have been used for the compilation of a new glacier inventory based on LiDAR DEMs (Abermann et al., 2010). As the high resolution data allow detailed mapping of LIA moraines, the unpublished maps of Groß have been used as the basis for an accurate mapping of the area and elevation of the LIA moraines, based on the LiDAR DEMS and the ice divides/glacier names used in the inventories GI I and GI II.

The pilot study of Abermann et al. (2009) in the Ötztal Alps identified a pronounced downwasting of glacier area, but differing for different size classes, and Auer et al. (2007) found remarkably different precipitation trends south and north of the main Alpine ridge. This raises several research questions: (i) is the increasing retreat rate found by Abermann valid for all Austrian glaciers, or are the reverse precipitation trends found by Auer (2007) also reflected by glacier retreat rates? (ii) How large are the current retreat rates compared to past retreat rates? and (iii) can we define a relation which allows the calculation of area decrease as a function of climate change?

In this study, the compilation of the glacier inventories of LIA maximum state (GI LIA) and 2006 (GI III) is presented together with a comparison of area losses in the period LIA–1969, 1969–1998 and 1998–2006 with the respective climatic changes as recorded in the HISTALP climate data (Auer et al., 2007). After a short description of the method developed by Abermann et al. (2010), the resulting losses of area are presented for the specific mountain ranges and size classes.

2 Data

This study is based on glacier inventory data of 1969 and 1998, updated by LiDAR data and orthophotos and compared with climatic changes since the LIA as documented by the high quality HISTALP instrumental climate data.

2.1 Glacier inventories 1969 and 1998

The glacier inventories 1969 (GI I) and 1998 (GI II) have been compiled from orthophotos dating from 1969 and the years between 1996 and 2002. In the first, analogue, evaluation of the 1969 orthophotos by Groß (1987) and Patzelt (1980), the area 1969 was determined as $541.7\,\text{km}^2$. Lambrecht and Kuhn estimated a homogenized area for 1998, which differed by only $1.2\,\text{km}^2$ from the recorded areas. They found a glacier area of $470.9\,\text{km}^2$ for the areas of different dates, and $469.7\,\text{km}^2$ for a homogenized area for the year 1998. The digital reanalysis of the inventory 1969 by Lambrecht and Kuhn (2007) found a total glacier area of $540\,\text{km}^2$. The glacier areas have been delineated manually (Lambrecht and Kuhn, 2007; Kuhn et al., 2008) as recommended by UNESCO (1970). The volume change was quantified as $4.9\,\text{km}^3$, corresponding to a mean elevation change of $-8.7\,\text{m}$ in 29 years, corresponding to $-0.3\,\text{m\,year}^{-1}$. About 3 % of the glacier area of 1969 have not been mapped and several very small glaciers were still missing in GI II.

2.2 LiDAR data

Airborne laser scanning is a highly accurate method for the determination of surface elevation in high spatial resolution, allowing the mapping of geomorphologic features, such as moraines (Sailer et al., 2014). The data were recorded between 2006 and 2012 in several campaigns covering most of the Austrian glaciers. The minimum point density is $1\,\text{point}/4\,\text{m}^2$. The vertical resolution ranges from few decametres to several centimetres, depending on slope and surface roughness (Sailer et al., 2014). The

flights were carried out during August and September, when snow cover was minimal and the glacier margins snow free.

The survey flights took place at different dates. The DEMs have been compiled from a single campaign so that the recorded glacier elevation corresponds to one date only, although the acquisition times of the DEMs differ for the specific mountain ranges. The sensors and requirements on point densities are listed in Table 1. Vertical and horizontal resolution also depends on slope and elevation, nominal mean values for flat areas are better than ±0.5 m (horizontal) and ±0.3 m (vertical) accuracy.

2.3 Orthophotos

Orthophotos have been used for the delineation of glacier margins where no LiDAR data have been available. All orthophotos used are RGB colour orthophotos with a nominal resolution of 20 cm × 20 cm. Orthophotos from 2009 were used for Ankogel-Hochalmspitzgruppe, Defreggergruppe, Glocknergruppe, Granatspitzgruppe, the western part of Schobergruppe and the East Tyrolean part of Venedigergruppe. The eastern part of Zillertaler Alpen, also the northern part of Venedigergruppe, located in Salzburg province, were made with orthophotos from the year 2007. Orthophotos from 2012 were used for Dachsteingruppe.

2.4 Climate data

Regional differences of glacial changes have been compared to monthly means of glacier related climate parameters such as air temperatures, sunshine duration or precipitation. Monthly homogenized records of climate data such as temperature, pressure, precipitation, sunshine and cloudiness have been compiled for the Greater Alpine Region (GAR) in the HISTALP database (HISTALP, 2014; Auer et al., 2007). These go back as far as 1760 and are available in station mode or as grid. Auer et al. (2007) identified incremental temperature increases in the 20th century (+1.2 °C) with one peak in the 1950s and a second increase starting in the 1970s (+1.3 °C/25 a). They found

a remarkable opposed development with 9 % precipitation increase in the NW vs. 9 % decrease in the SE. For the comparison with the inventory data, mean temperatures and sunshine duration during the ablation season (May to September) were analysed as well as precipitation in the accumulation season (October of the previous year to April of the current year).

Ten stations in Austria, one in Italy and two in Eastern Switzerland (Begert et al., 2005) have been selected to represent climate and climate change in Austria's glacier covered regions for the following criteria: (i) length of record, (ii) availability of parameters, and (iii) location within or close to specific glacier regions or shown correlation with glacier mass balance in the region (Fig. 1, Table 2).

3 Method

3.1 Applied basic definitions

As the compilation of the glacier inventory time series aims to allow monitoring any changes, several definitions and parameters have been kept unchanged between the inventories, although they could have been changed for compiling single inventories. To make the definitions clear, the definition of glaciers, as well as glacier area and the separation by ice divides are specified here.

The glacier inventory of 1969 Patzelt (1980) contained a number of geomorphological parameters, such as aspect, type, minimum and maximum elevations, and the ELA, as well as two different definitions of glacier areas: the area in 1969 was recorded with and without non-moving parts above the bergschrunds. The inventory of 1969 was partly reanalysed during the compilation of the glacier inventory of 1998 (Lambrecht and Kuhn, 1998), adding snow covered area connected to the glacier to the glacier area, as it is impossible to prove if the snow covers ice or ground. Geomorphological parameters are only available for the inventory of 1969.

A. Fischer et al.

A consistent definition of specific glacier area between the LIA inventory and later inventories is not straightforward, as often several glaciers joined in one glacier tongue during LIA, but split up in later inventories. To avoid confusion, unique IDs in the glacier inventory of 1969 and 1998 have been kept, even if the glacier had disintegrated in the inventory of 2006, so that one ID can refer to polygons consisting of several parts of a formerly connected glacier area. For the comparison of LIA areas on the basis of individual glaciers, the LIA glaciers have not been divided because the position of medial moraines remains unclear, but these LIA glaciers have been compared to all glaciers that are part of the LIA area today.

The ice divides remain unchanged in all glacier inventories and are defined from the glacier surface in 1998. Although ice dynamics are likely to change between the inventories, leaving the position of the divides unchanged has the advantage that no area has shifted from one glacier to another.

The manual delineation of the glacier areas in GI III avoids major problems with the identification if debris-covered glacier parts, because the combination of volume change, surface roughness and optical images from various sources allows the identification of debris-covered parts of the glaciers by the subsidence of the surface.

No size limit was applied for the mapping of glaciers in the inventory 2006, i.e. glaciers whose area has shrunk below a certain limit are still included in the updated inventory. This avoids an overestimate of the total loss of ice-covered area as a result of skipping small glaciers included in older inventories.

3.2 Mapping of glacier extent 2006 from LiDAR

The point density in one grid cell of $1\,m \times 1\,m$ ranges from 0.25 to 1 point per square metre. The vertical accuracy depends on slope and surface roughness and ranges from few cm to some dm in very steep terrain (Sailer et al., 2014). LiDAR has a considerable advantage over photogrammetry where fresh snow or shading reduce accuracy. As the high spatial resolution also reflects surface roughness, smooth ice-covered surfaces can be clearly distinguished from rough periglacial terrain. Abermann et al. (2010)

demonstrated in a pilot study for the Ötztal Alps that LiDAR DEMs can be used with high accuracy for mapping glacier area. The update of the glacier shapes from the inventory of 1998 was done combining hill shades with different angles calculated from LiDAR DEMs, analysing the surface elevation changes between the GI I and GI II invento- ries and by comparison with orthophoto data, where available. Abermann et al. (2010) quantify the accuracy of the areas derived by their method to ±1.5 % for glaciers larger than 1 km^2 and up to ±5 % for smaller ones. The comparison with glacier margins mea- sured by DGPS in the field for 118 points showed that 95 % of these glacier margins derived from LiDAR were within an 8 m radius of the measured points and 85 % within a 4 m radius.

3.3 Deriving the LIA extent

LIA extents have been calculated by Groß (1987), who also summarized available his- torical documents and maps. Richter's glacier inventory of 1888 was based on military maps, which were certainly a milestone in cartography at that time, but showed great uncertainties regarding the extent of the firn areas. Groß (1989) and Patzelt (1973) mapped the LIA extents of 85 % of the Austrian glaciers based on field surveys and the maps and orthophotos of the 1969 glacier inventory. As the spatial resolution of the new LiDAR DEMs is high, the position of the LIA moraines is reproduced much more accurately than in previously available elevation models. In addition to that, the analogue glacier margin maps had been stored for several decades and suffered some distortion of the paper, so that the digitalization could not reproduce the accurate po- sition of the glacier tongues according to the LiDAR DEMs. Therefore we decided to remap the LIA glacier areas, basically following the interpretation of Groß and Patzelt, but remaining consistent with the digital data.

Nevertheless, some smaller glaciers, which had wasted down until 1969, might still be missing in the LIA inventory. Groß (1987) accounted for these disappeared glaciers by adding 6.5 % to the LIA area. We decided to include this consideration in the dis- cussion on uncertainties, although we think that this estimate is fairly accurate.

3.4 Climate records

The monthly homogenized data were analysed with reference to the typical extent of accumulation and ablation seasons in the Austrian Alps, i.e. from the beginning of October to the end of April for accumulation (precipitation sums) and from the beginning of May to the end of September for ablation (mean air temperatures and sunshine duration). To separate long-term climate change within the periods of the glacier inventories, a 30 year running mean centred on the final year of the period was chosen. This method seems to be less influenced by singular extreme values than linear trend analysis.

4 Results

In GI III, glaciers cover 415.11 km^2, equivalent to 44 % of the glacier area at the LIA maximum determined in this study (941.13 km^2 without disappeared glaciers, which is a bit lower than the 945.50 km^2 found by Groß, 1987). Only four glaciers have wasted down completely since GI II. The loss of area between GI II and GI III is 55.97 km^2, which is more than half of the area loss of −94.21 km^2 in the 29 years between acquisition of GI I and GI II. Annual area losses are highest in the latest period (GI II to GI III: 0.23 km^2 year^{-1}). Losses between LIA and GI I (−0.16 km^2 year^{-1}) exceeded the ones between GI I and GI II (0.13 km^2 year^{-1}). The relative annual area loss was only 0.02 % until GI II, rising to 0.05 % year^{-1} for the latest period.

The areas recorded for specific mountain ranges are shown in Fig. 2 and Table 3. Highest absolute glacier area decrease between GI II and GI III was observed in the Ötztal Alps (−13.94 km^2, 24 % of total area loss), the Venedigergruppe (−11.70 km^2, 20.9 % of total area loss), Stubaier Alpen (8.20 km^2, 4.5 %) and Glocknergruppe (−8.17 km^2, 14.6 % of total area loss). These mountain ranges contribute 74.2 % of the total Austrian glacier area. Their contribution to the area loss is lower than their share of glacier area, and is only 60.4 % of the area loss. The contribution of the Ötztaler Alpen,

Silvretta, Zillertaler Alpen and Stubaier Alpen to the total Austrian area loss decreased between the LIA and today, the contribution of Glocknergruppe and Venedigergruppe increased by more than 4 % of the total area loss for each mountain range. The regional variability of the relative annual area loss in the period GI II to GI III is high. The maximum relative annual area loss was observed in the Salzburger Kalkalpen, where the disintegration of the Übergossene Alm glacier results in a relative loss as high as 7.8 % of the glacier area per year. While in most of the mountain ranges about 1 % of the total glacier area is lost per year, in mountain ranges covered by smaller glaciers, such as Allgäuer Alpen, Karnische Alpen, Samnaun and Verwallgruppe, the annual losses may exceed 4 % of the total glacier area. During earlier periods, the relative losses did not exceed 1 %, although the evaluation of shorter periods might of course reveal higher rates which would be smoothed in longer periods.

The area loss since the LIA maximum differs between the specific groups: whereas only 11 % of the LIA area is left in the Samnaun Gruppe, 51 to 45 % of the LIA area is still ice covered in Rätikon, Ötztaler Alpen, Venedigergruppe, Silvretta, Glocknergruppe and Stubaier Alpen (Fig. 3).

4.1 Altitudinal variability of area changes

In GI II, 88 % of the total area was located at elevations between 2600 and 3300 m a.s.l. (Fig. 4). In GI II, the proportion of glacier area located at these elevations was still 87 %. The largest portion of the area is located at elevations between 2850 and 3300 m a.s.l. (41 % in GI II and 58 % in GI III), 42 % of the area was located in regions above 3000 m in GI II, decreasing to 39 % in GI III:

The most severe losses took place in altitudinal zones between 2650 and 2800 m a.s.l., with a maximum in the elevation zone 2700 to 2750 m a.s.l. 50 % of the area losses took place at altitudes between 2600 and 2900 m a.s.l. Therefore the main portion of the glaciated areas are stored in regions above the current strongest area retreats.

4.2 Area changes for specific glacier sizes

The interpretation of the recorded glacier sizes has to take into account that not all glaciers which are mapped for newer inventories are part of the older inventories, as the total number of glaciers in Table 4 shows. Although some smaller glaciers are missing in GI I, the number of glaciers smaller than $0.1\,\text{km}^2$ has been increasing, replacing the area class between 0.1 and $0.5\,\text{km}^2$ as the most frequent one. At the other end of the scale, 11 glaciers had been part of the largest size class in GI I, of which only 8 were left in GI III.

For GI III, the glaciers in size class $5\text{--}10\,\text{km}^2$ cover 41 % of the area, which is the largest size class (Table 5). All other size classes range between 8 and 17 % of the total area, but glaciers of the smallest size class cover only 9 % of the total glacier area.

4.3 Climate change

Long-term climate records show an increase of air temperature since the end of the LIA, more pronounced since 1983, when the 30 year running mean was at a minimum for the years after 1942 at low elevations (Fig. 5). Sunshine duration shows the same minima in the early 1980s for all stations, the early 1940s minima occur in the two stations at low elevations. In contrast to the low elevation stations, the mountain stations Zugspitze and Sonnblick recorded an increase of average air temperature and sunshine duration without a pronounced minimum at the beginning of the 1940s.

Regional variability of precipitation – as described by Auer (2007) – is higher than for air temperatures. The inner-Alpine stations show an increase in precipitation in the 1930s to 1940s. A maximum of the running mean in the early 1970s has been observed in Linz, Kremsmünster and Rauris, i.e. in the northeast, but not for the inner-Alpine and southern stations. Increases in winter precipitation from around the year 2000 have been most pronounced in the north, and less so south of the main Alpine ridge. The mean values of summer temperatures, winter precipitation and sunshine duration for the inventory periods are presented in Table 6.

Tracing glacial disintegration from the LIA to the present using a LIDAR-based glacier inventory

A. Fischer et al.

Title Page

Abstract | Introduction

Conclusions | References

Tables | Figures

|◄ | ►|

◄ | ►

Back | Close

Full Screen / Esc

Printer-friendly Version

Interactive Discussion

5   Discussion

The uncertainties of the derived glacier areas are estimated to be highest for the LIA inventory, and lowest for GI III. For all glacier inventories, debris cover and perennial snow fields or fresh snow patches connected to the glacier are hard to identify, although including information on high resolution elevation changes and including additional information from different points in time reduces this uncertainty (Abermann et al., 2010). The high-resolution data were only available for GI III, so that the interpretation of debris and snow can still be regarded as an interpretational range of several percentage points for the area in GI I and II. The nominal accuracy of the method (Abermann et al., 2010) results in an area uncertainty of $\pm 11.17\,\mathrm{km}^2$ or 2.69 %.

For the interpretation of the LIA inventory, temporal and spatial indeterminacy has to be kept in mind. The temporal indeterminacy is caused by the asynchronous occurrence of the LIA maximum extent. In extreme cases the occurrence of the LIA maximum deviated several decades from the year 1850, which is often used as synonymous with the time of the LIA maximum.

The spatial indeterminacy varies between accumulation areas and glacier tongues: the moraines which confined the LIA glacier tongues give a good indication for the LIA glacier margins in most cases as they are clearly mapped in the LiDAR DEMs and changing vegetation is visible in the orthophotos. In some cases, lateral moraines standing proud for several decades eroded later, so that the LIA glacier surface will be interpreted as wider, but also lower than it actually was. In some cases, LIA moraines were subject to mass movements caused by fluvial or permafrost activities. In a very few cases, ice cored moraines developed and moved from the original position. Altogether these uncertainties are small compared to the interpretational range at higher elevations, where no significant LIA moraines indicate the ice margins. Moreover, historical documents and maps often show fresh or seasonal snow cover at higher elevations. Therefore we cannot even be sure to have included all glaciers which existed during the LIA maximum, as it is impossible to distinguish perennial snow fields from

glacial firn. Assuming, as is the case in later inventories, that the ice cover at high elevations is small as a result of wind drift and avalanche activity, we estimate the accuracy of the total ice cover for the LIA as ±10 %.

In any investigation of large system changes, as between LIA and today, the definition of the term "glacier" is difficult, but necessary if we aim at further modelling of parameters such as mass balance or ice thickness involving glacier dynamics. Calculating ice divides from surface DEMs for every inventory does not allow deriving glacier statistics, as ice divides and therefore glacier areas change too much. The disintegration of glaciers after the LIA could be captured best by using parent-and-child IDs, but so far no systematics have been established in the international community.

Regarding the presented annual rates of area change, it has to be born in mind that all periods apart from GI II to GI III contain at least one period (around 1920 and in the 1980s) when the majority of glaciers advanced. Thus a higher temporal resolution of inventories might result in different annual area change rates, as the length change rates, for example during the 1940s, have been in the same dimension as those after 2000.

Groß (1987) calculated glacier areas for 1850 (945.50 km^2 without, and 1011.00 with disappeared glaciers), 1920 (758.60 km^2) and 1969 (541.73 km^2). A reconstruction of glacier areas for 1920 has not been attempted within this study. The figures of Groß (1987) for the glacier area in 1969 differ slightly from those given by Lambrecht and Kuhn (2007) and from those in this study, as snow patches connected with the glacier have been neglected. In order to avoid having to reanalyse the digital data compiled by Lambrecht and Kuhn (2007), the authors stuck to the same definition of glaciers as Lambrecht and Kuhn (2007). For the last decade, changes would only have amounted to 3 % maximum, as a series of negative mass balance years has significantly reduced perennial snow patches.

The application of a minimum glacier size would lead to a significant decrease in the number of Austrian glaciers and of course also to a reduction of glacier area. As

this study wanted to trace the changes in glacier area, no minimum glacier size was applied.

The development of area change rates is similar to the ones found for the Aosta region by Diolaiuti et al. (2012), who arrived at 2.8 km^2 year^{-1} for 1999 to 2005, and 1.1 km^2 year^{-1} for 1975 to 1999. The maximum relative area changes in the period of the Austrian GI II to GI III exceed the ones summarized by Gardent et al. (2014). The periods for which area changes have been calculated for the French Alps by Gardent et al. (2014) are no exact match of the Austrian periods, but the total loss of 25.4 % of the glacier area between 1967/71 and 2006/09 is similar to the Austrian Alps, despite the higher elevations of the French glaciers. A common finding is the high regional variability of the area changes.

Compared to remote-sensing-based glacier inventories of the area, the glacier inventories presented here have the advantage of (i) higher spatial resolution (ii) inclusion of additional information (iii) minimal snow cover at the time of the flights and (iv) consistent nomenclature and ice divides for all four inventories. The comparison with the Randolph inventory RGI Version 3.2 (Arendt et al., 2012), released 6 September 2013 and downloaded from http://www.glims.org/RGI/rgi_dl.html shows that the number of RGI glaciers (737) as well as the glacier area of 363.877 km^2 for the year 2003 is lower than the glacier area recorded in the Austrian inventories (GI II before 2003 and GI III after 2003), although cross-border glaciers have not been delimited for the comparison. This shows the importance of consistent data management for deriving time series of inventories.

For the statistics on the number of glaciers, and therefore parameters such as the mean glacier size, a homogenous definition of a glacier as connected area together with a name convention would be an advantage, especially when comparing LIA glaciers with their split remnants of today.

6   Conclusions

This time series of glacier inventories presents a unique document of glacier area change since the Little Ice Age. The regional variability of glacier area loss is high, ranging from 11 % of the LIA glacier area still left for the small glaciers of the Samnaun group to half of the glacier area left for a number of other groups. For some regions, like the Salzburger Kalkalpen, the plateau glacier seems likely to vanish in the near future. Nevertheless, for most regions the annual losses do not exceed 4 %. Between GI I and GI II, the loss rates were below 1 %, so that the relative losses after 2000 have been rising. However, it must be taken into account that this period is rather shorter than the others and lacks glacier advances.

The comparison of area changes with changes in climate reveals that not only climate, but also the topography and glacier states, might play an important role. The significant temperature increase for the recent period GI II to GI III is reflected in an increase of area losses. The influence of regional differences in winter precipitation could not be traced back to area changes, as glacier sizes and accumulation situation might differ too much between the regions.

The compilation of time series of glacier inventories shows up the need for consistent definitions and IDs. The disintegration of glaciers, along with the separation of glacier tributaries, can only be handled with a standardized system of parent-and-child IDs that allow the prolongation of time series into the future and the past. This is especially important for the application of numerical models that include ice dynamics for volume calculations.

Further investigation will show if the proposed relation between mean changes in summer temperatures and area change is a reliable guide for other regions and/or time periods. The analysis of the regional variability of volume changes, together with temperature and precipitation anomalies, will be the next step to fully exploit the presented time series of glacier inventories.

References

Abermann, J., Lambrecht, A., Fischer, A., and Kuhn, M.: Quantifying changes and trends in glacier area and volume in the Austrian Ötztal Alps (1969-1997-2006), The Cryosphere, 3, 205–215, doi:10.5194/tc-3-205-2009, 2009.

Abermann, J., Fischer, A., Lambrecht, A., and Geist, T.: On the potential of very high-resolution repeat DEMs in glacial and periglacial environments, The Cryosphere, 4, 53–65, doi:10.5194/tc-4-53-2010, 2010.

Andreassen, L. M., Paul, F., Kääb, A., and Hausberg, J. E.: Landsat-derived glacier inventory for Jotunheimen, Norway, and deduced glacier changes since the 1930s, The Cryosphere, 2, 131–145, doi:10.5194/tc-2-131-2008, 2008.

Arendt, A., Bolch, T., Cogley, J. G., Gardner, A., Hagen, J.-O., Hock, R., Kaser, G., Pfeffer, W. T., Moholdt, G., Paul, F., Radić, V., Andreassen, L., Bajracharya, S., Barrand, N., Beedle, M., Berthier, E., Bhambri, R., Bliss, A., Brown, I., Burgess, D., Burgess, E., Cawkwell, F., Chinn, T., Copland, L., Davies, B., De Angelis, H., Dolgova, E., Filbert, K., Forester, R., Fountain, A., Frey, H., Giffen, B., Glasser, N., Gurney, S., Hagg, W., Hall, D., Haritashya, U. K., Hartmann, G., Helm, C., Herreid, S., Howat, I., Kapustin, G., Khromova, T., Kienholz, C., Köonig, M., Kohler, J., Kriegel, D., Kutuzov, S., Lavrentiev, I., LeBris, R., Lund, J., Manley, W., Mayer, C., Miles, E., Li, X., Menounos, B., Mercer, A., Mölg, N., Mool, P., Nosenko, G., Negrete, A., Nuth, C., Pettersson, R., Racoviteanu, A., Ranzi, R., Rastner, P., Rau, F., Raup, B., Rich, J., Rott, H., Schneider, C., Seliverstov, Y., Sharp, M., Sigurðsson, O., Stokes, C., Wheate, R., Winsvold, S., Wolken, G., Wyatt, F., and Zheltyhina, N.: Randolph Glacier Inventory – a Dataset of Global Glacier Outlines: Version 3.2, Global Land Ice Measurements from

Space, Boulder, Colorado, USA, Digital Media, http://www.glims.org/RGI/rgi_dl.html (last access: 15 July 2014), 2012.

Auer, I., Böhm, R., Jurkovic, A., Lipa, W., Orlik, A., Potzmann, R., Schöner, W., Ungersböck, M., Matulla, C., Briffa, K., Jones, P. D., Efthymiadis, D., Brunetti, M., Nanni, T., Maugeri, M.,
5 Mercalli, L., Mestre, O., Moisselin, J.-M., Begert, M., Müller-Westermeier, G., Kveton, V., Bochnicek, O., Stastny, P., Lapin, M., Szalai, S., Szentimrey, T., Cegnar, T., Dolinar, M., Gajic-Capka, M., Zaninovic, K., Majstorovic, Z., and Nieplova, E.: HISTALP – historical instrumental climatological surface time series of the greater Alpine region 1760–2003, Int. J. Climatol., 27, 17–46, 2007.

10 Begert, M., Schlegel, T., and Kirchhofer, W.: Homogeneous temperature and precipitation series of Switzerland from 1864 to 2000, Int. J. Climatol., 25, 65–80, 2005.

Bolch, T., Yao, T., Kang, S., Buchroithner, M. F., Scherer, D., Maussion, F., Huintjes, E., and Schneider, C.: A glacier inventory for the western Nyainqentanglha Range and the Nam Co Basin, Tibet, and glacier changes 1976–2009, The Cryosphere, 4, 419–433, doi:10.5194/tc-
15 4-419-2010, 2010.

Diolaiuti, G. A., Bocchiola, D., Vagliasindi, M., D'Agata, C., and Smiraglia, C.: The 1975–2005 glacier changes in Aosta Valley (Italy) and the relations with climate evolution Prog. Phys. Geogr., 36, 764–785, doi:10.1177/0309133312456413, 2012.

Fischer, M., Huss, M., and Hoelzle, M.: Surface elevation and mass changes of all Swiss
20 glaciers 1980–2010, The Cryosphere Discuss., 8, 4581–4617, doi:10.5194/tcd-8-4581-2014, 2014.

Gardent, M., Rabatel, A., Dedieu, J.-P., and Deline, P.: Multitemporal glacier inventory of the French Alps from the late 1960s to the late 2000s, Global Planet. Change, 120, 24–37, doi:10.1016/j.gloplacha.2014.05.004, 2014.

25 Gardner, A. S., Moholdt, G., Cogley, G., Wouters, B., Arendt, A. A., Wahr, J., Berthier, E., Hock, R., Pfeffer, W. T., Kaser, G., Ligtenberg, S. R. M., Bolch, T., Sharp, M. J., Hagen, J. O., van den Broeke, M. R., and Paul, F.: A reconciled estimate of glacier contributions to sea level rise: 2003 to 2009, Science, 340, 852–857, doi:10.1126/science.1234532, 2013.

Gross, G.: Der Flächenverlust der Gletscher in Österreich 1850-1920-1969, Z. Gletscherk.
30 Glazialgeol., 23, 131–141, 1987.

Hagg, W., Mayer, C., Mayr, E., and Heilig, A.: Climate and glacier fluctuations in the Bavarian Alps during the past 120 years, Erdkunde, 66, 121–142, 2012.

Title Page

Abstract | Introduction

Conclusions | References

Tables | Figures

◄ | ►

◄ | ►

Back | Close

Full Screen / Esc

Printer-friendly Version

Interactive Discussion

Haggren, H., Mayer, C., Nuikka, M., Rentsch, H., and Peipe, J.: Processing of old terrestrial photography for verifying the 1907 digital elevation model of Hochjochferner Glacier, Z. Gletscherk. Glazialgeol., 41, 29–53, 2007.

HISTALP: Climate Data, available at: http://www.zamg.ac.at/histalp, last access: 14 July 2014.

Huss, M.: Extrapolating glacier mass balance to the mountain-range scale: the European Alps 1900–2100, The Cryosphere, 6, 713–727, doi:10.5194/tc-6-713-2012, 2012.

Huss, M. and Farinotti, D.: Distributed ice thickness and volume of all glaciers around the globe, J. Geophys. Res., 117, F04010, doi:10.1029/2012JF002523, 2012.

Jarvis, A., Reuter, H. I., Nelson, A., and Guevara, E.: Hole-filled seamless SRTM data V4, International Centre for Tropical Agriculture (CIAT), available from: http://srtm.csi.cgiar.org (last access: October 2014), 2008.

Kääb, A., Paul, F., Maisch, M., Hoelzle, M., and Haeberli, W.: The new remote sensing derived Swiss glacier inventory: II. First results, Ann. Glaciol., 34, 362–366, 2002.

Kargel, J. S., Leonard, G. J., Bishop, M. P., Kaab, A., and Raup, B. (Eds.): Global Land Ice Measurements from Space, Springer-Praxis, Berlin, Heidelberg, 2014.

Knoll, C. and Kerschner, H.: A glacier inventory for South Tyrol, Italy, based on airborne laserscanner data, Ann. Glaciol., 50, 46–52, 2010.

Kuhn, M., Lambrecht, A., Abermann, J., Patzelt, G., and Groß, G.: Die österreichischen Gletscher 1998 und 1969, Flächen und Volumenänderungen, Verlag der Österreichischen Akademie der Wissenschaften, Wien, 2008.

Lambrecht, A. and Kuhn, M.: Glacier changes in the Austrian Alps during the last three decades, derived from the new Austrian glacier inventory, Ann. Glaciol., 46, 177–184, 2007.

Linsbauer, A., Paul, F., and Haeberli, W.: Modeling glacier thickness distribution and bed topography over entire mountain ranges with Glab-Top: application of a fast and robust approach, J. Geophys. Res., 117, F03007, doi:10.1029/2011JF002313, 2012.

López-Moreno, J. I., Fontaneda, S., Bazo, J., Revuelto, J., Azorin-Molina, C., Valero-Garcés, B., Morán-Tejeda, E., Vicente-Serrano, S. M., Zubieta, R., and Alejo-Cochachín, J.: Recent glacier retreat and climate trends in Cordillera Huaytapallana, Peru, Global Planet. Change, 112, 1–11, doi:10.1016/j.gloplacha.2013.10.010, 2014.

Maisch, M., Wipf, A., Denneler, B., Battaglia, J., and Benz, C.: Die Gletscher der Schweizer Alpen, Gletscherhochstand 1850 – Aktuelle Vergletscherung – Gletscherschwund-Szenarien 21. Jahrhundert, vdf Hochschulverlag an der ETH Zürich, Zürich, 1999.

Title Page

Abstract | Introduction

Conclusions | References

Tables | Figures

|◀ | ▶|

◀ | ▶

Back | Close

Full Screen / Esc

Printer-friendly Version

Interactive Discussion

Marzeion, B., Jarosch, A. H., and Hofer, M.: Past and future sea-level change from the surface mass balance of glaciers, The Cryosphere, 6, 1295–1322, doi:10.5194/tc-6-1295-2012, 2012.

Müller, F., Caflisch, T., and Müller, G.: Firn und Eis der Schweizer Alpen, Gletscherinventar, Eidgenössische Technische Hochschule, Geographisches Institut Publ. 57 and 57a, Zürich, 1976.

Nuth, C., Kohler, J., König, M., von Deschwanden, A., Hagen, J. O., Kääb, A., Moholdt, G., and Pettersson, R.: Decadal changes from a multi-temporal glacier inventory of Svalbard, The Cryosphere, 7, 1603–1621, doi:10.5194/tc-7-1603-2013, 2013.

Ohmura, A.: Enhanced temperature variability in high-altitude climate change, Theor. Appl. Climatol., 110, 499–508, 2012.

Patzelt, G.: Die neuzeitlichen Gletscherschwankungen in der Venedigergruppe (Hohe Tauern, Ostalpen), Z. Gletscherk. Glazialgeol., 9, 5–57, 1973.

Patzelt, G.: The Austrian Glacier inventory: status and first results, IAHS-AISH P., 126, 181–183, 1980.

Paul, F. and Haeberli, W.: Spatial variability of glacier elevation changes in the Swiss Alps obtained from two digital elevation models, Geophys. Res. Lett., 35, L21502, doi:10.1029/2008GL034718, 2008.

Paul, F., Kääb, A., Maisch, M., Kellenberger, T., and Haeberli, W.: Rapid disintegration of Alpine glaciers observed with satellite data, Geophys. Res. Lett., 31, L21402, doi:10.1029/2004GL020816, 2004.

Paul, F., Barry, R. G., Cogley, J. G., Frey, H., Haeberli, W., Ohmura, A., Ommanney, C. S. L., Raup, B., Rivera, A., and Zemp, M.: Guidelines for the compilation of glacier inventory data from digital sources, Ann. Glaciol., 50, 119–126, 2010.

Paul, F., Andreassen, L. M., and Winsvold, S. H.: A new glacier inventory for the Jostedalsbreen region, Norway, from Landsat TM scenes of 2006 and changes since 1966, Ann. Glaciol., 52, 153–162, 2011a.

Paul, F., Frey, H., and Le Bris, R.: A new glacier inventory for the European Alps from Landsat TM scenes of 2003: Challenges and results, Ann. Glaciol., 52, 144–152, 2011b.

Paul, F., Barrand, N., Berthier, E., Bolch, T., Casey, K., Frey, H., Joshi, S. P., Konovalov, V., Le Bris, R., Moelg, N., Nosenko, G., Nuth, C., Pope, A., Racoviteanu, A., Rastner, P., Raup, B., Scharrer, K., Steffen, S., and Winsvold, S.: On the accuracy of glacier outlines derived from remote sensing data, Ann. Glaciol., 53, 171–182, 2013.

Title Page

Abstract | Introduction

Conclusions | References

Tables | Figures

◄ | ►

◄ | ►

Back | Close

Full Screen / Esc

Printer-friendly Version

Interactive Discussion

Radić, V. and Hock, R.: Regional and global volumes of glaciers derived from statistical upscaling of glacier inventory data, J. Geophys. Res., 115, F01010, doi:10.1029/2009JF001373, 2010.

Radić, V. and Hock, R.: Regionally differentiated contribution of mountain glaciers and ice caps to future sea-level rise, Nat. Geosci., 4, 91–94, doi:10.1038/ngeo1052, 2011.

Rott, H.: Analyse der Schneeflächen auf Gletschern der Tiroler Zentralalpen aus Landsat-Bildern, Z. Gletscherk.d Glazialgeol., 12/1, 1–28, 1977.

Sailer, R., Rutzinger, M., Rieg, L., and Wichmann, V.: Digital elevation models derived from airborne laser scanning point clouds: appropriate spatial resolutions for multi-temporal characterization and quantification of geomorphological processes, Earth Surf. Proc. Land., 39, 272–284, doi:10.1002/esp.3490, 2014.

UNESCO: Perennial Ice and Snow Masses: a Guide for Compilation and Assemblage of Data for a World Inventory, Tech. Pap. Hydrol. 1., UNESCO/IASH, Paris, 1970.

Vaughan, D. G., Comiso, J. C., Allison, I., Carrasco, J., Kaser, G., Kwok, R., Mote, P., Murray, T., Paul, F., Ren, J., Rignot, E., Solomina, O., Steffen, K., and Zhang, T.: Observations: cryosphere, in: Climate Change 2013: The Physical Science Basis, Contribution of Working Group I to the Fifth Assessment Report of the Intergovernmental Panel on Climate Change, edited by: Stocker, T. F., Qin, D., Plattner, G.-K., Tignor, M., Allen, S. K., Boschung, J., Nauels, A., Xia, Y., Bex, V., and Midgley, P. M., Cambridge University Press, Cambridge, UK and New York, NY, USA, 2013.

WGMS, and National Snow and Ice Data Center (comps.): World Glacier Inventory, National Snow and Ice Data Center, Boulder, Colorado, USA, doi:10.7265/N5/NSIDC-WGI-2012-02, 1999, updated 2012.

Table 1. Sensor and point densities.

	Sensor	Point density m^{-2}
Tyrol	ALTM 3100 and Gemini	0.25
Salzburg	Leica ALS-50, Optech ALTM-3100	1.00
Vorarlberg	ALTM 2050	2.50
Carinthia-Karnische Alpen	Riegl LMS Q680i and Riegl LMS Doublescansystem	1.00
Carinthia-other	Leica ALS-50/83 and Optech Gemini	1.00

Table 2. List of climate stations with available parameters and the first recorded year. p: precipitation, t: temperature, s: sunshine duration.

Station name	Long.	Lat.	Height	1st recorded year		
	E	N	m a.s.l.	p	t	s
Innsbruck	11.385	47.261	609	1858	1777	1906
Kötschach-Mauthen	12.998	46.678	714	1871		
Kremsmünster	14.131	48.055	382	1820	1767	1884
Linz-Stadt	14.286	48.297	263	1852	1816	
Mariapfarr	13.745	47.152	1153			1930
Marienberg/Montemaria	10.490	46.740	1323	1858	1858	
Patscherkofel	11.462	47.210	2247		1931	1935
Rauris	12.993	47.224	941	1876	1876	
Sonnblick	12.958	47.054	3105		1887	1887
Villacher Alpe	13.673	46.604	2160			1884
Zugspitze	10.980	47.420	2962		1901	1901
Davos	9.843	46.813	1594	1866	1866	
Säntis	9.343	47.250	2502	1882	1864	

Table 3. Acquisition times of the glacier inventories with glacier areas for specific mountain ranges shown in Fig. 1; L means LiDAR ALS data and O means orthophoto.

Group	GI II year	GI III year	Data source	LIA km^2	GI-I km^2	GI-II km^2	GI-III km^2
Allgäuer Alpen	1998	2006	L	0.29	0.20	0.09	0.07
Ankogel-Hochalmspitzgruppe	1998	2009	O	39.94	19.17	16.03	12.05
Dachsteingruppe	2002	2012	O	11.95	6.28	5.69	5.08
Defregger Gruppe	1998	2009	O	2.01	0.70	0.43	0.30
Glocknergruppe	1998	2009	O	103.58	68.93	59.84	51.67
Granatspitzgruppe	1998	2009	O	20.08	9.76	7.52	5.48
Karnische Alpen	1998	2009	L	0.29	0.20	0.18	0.09
Lechtaler Alpen	1996	2004/2006	L	2.09	0.70	0.69	0.55
	1996	2006	L				0.36
	1996	2004	L				0.19
Ötztaler Alpen	1997	2006	L	280.35	178.32	151.16	137.58
Rätikon	1996	2004	L	3.12	2.19	1.65	1.61
Rieserfernergruppe	1998	2009	L	8.07	4.60	3.13	2.75
Salzburger Kalkalpen	2002	2007	L	5.68	2.47	1.68	1.16
Samnaungruppe	2002	2006	L	0.59	0.20	0.08	0.07
Schobergruppe	1998	2007/2009	L/O	9.88	5.60	3.49	2.57
	1998	2007	L				0.96
	1998	2009	O				1.61
Silvrettagruppe	1996	2004/2006	L	41.27	23.96	18.97	18.48
		2006	L				9.86
		2004	L				8.62
Sonnblickgruppe	1998	2009	L	24.81	12.76	9.74	7.91
Stubaier Alpen	1997	2006	L	110.10	63.05	53.99	49.42
Venedigergruppe	1997	2007/2009	L/O	145.20	93.44	81.01	69.31
	1997	2007	O				29.85
	1997	2009	L				39.47
Verwallgruppe	2002	2004/2006	L	13.41	6.70	4.65	4.08
	2002	2006	L				3.66
	2002	2004	L				0.41
Zillertaler Alpen	1999	2007/2011	L/O	118.42	65.64	50.64	45.24
	1999	2007	O				4.73
	1999	2011	L				40.51
total area				941.13	564.88		470.67	415.47
% of LIA area				100.00	60.02		50.01	44.15

Discussion Paper | Discussion Paper | Discussion Paper | Discussion Paper |

TCD

8, 5195–5226, 2014

Tracing glacial disintegration from the LIA to the present using a LIDAR-based glacier inventory

A. Fischer et al.

Title Page

Abstract | Introduction

Conclusions | References

Tables | Figures

|◄ | ►|

◄ | ►

Back | Close

Full Screen / Esc

Printer-friendly Version

Interactive Discussion

Table 4. Number of glaciers by size classes.

Size classes [km^2]	< 0.1	0.1 to 0.5	0.5 to 1	1 to 5	5 to 10	> 10	Total
number of glaciers							
in GI I	177	401	116	99	11	5	809
in GI II	401	343	92	79	7	3	925
in GI III	450	307	77	77	8	2	921

Table 5. Distribution of area for different size classes.

	in % of total area		
	GI I	GI II	GI III
< 0.1 km^2	2	4	5
0.1 to 0.5 km^2	17	17	17
0.5 to 1.0 km^2	15	14	12
1 to 5 km^2	40	41	41
5 to 10 km^2	14	14	17
10 to 50 km^2	13	10	8

Table 6. Mean summer air temperatures, sunshine duration and winter precipitation sums for the glacier inventory periods.

Precipitation 1 Oct–30 Apr	1850–1969	1970–1998 mm	1999–2006 mm
Innsbruck		343	405
Kötschach-Mauthen		594	729
Kremsmünster		451	517
Linz-Stadt		421	466
Marienberg/Montemaria		287	332
Rauris		435	424
Davos		428	467
Säntis		1544	1549
air temperature 1 May–30 Sep	1850–1969 °C	1970–1998 °C	1999–2006 °C
Innsbruck	15.3	16.0	17.2
Kremsmünster	15.6	16.2	17.1
Linz-Stadt	16.0	16.6	17.9
Marienberg/Montemaria		12.2	13.4
Patscherkofel		5.5	6.7
Rauris		12.2	13.3
Sonnblick		0.0	1.0
Zugspitze		0.5	1.5
Davos		9.4	10.6
Säntis		3.2	4.5
sunshine duration 1 May–30 Sep	1850–1969	1970–1998 hours	1999–2006 hours
Innsbruck		201	215
Kremsmünster		209	171
Mariapfarr		180	190
Patscherkofel		184	199
Sonnblick		147	159
Villacher Alpe		185	208
Zugspitze		162	171

Title Page

Abstract | Introduction

Conclusions | References

Tables | Figures

|◄ | ►|

◄ | ►

Back | Close

Full Screen / Esc

Printer-friendly Version

Interactive Discussion
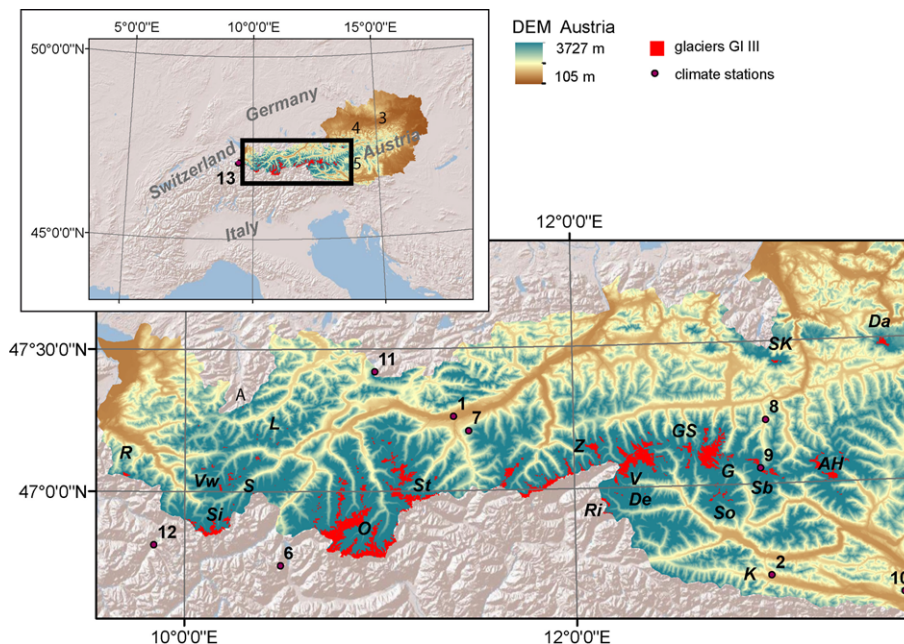
Figure 1. Austrian glaciers displayed on an elevation model (Jarvis et al., 2008) with mountain ranges and the acquisition dates of the LiDAR data as well as position of the climate stations. A: Allgäuer Alpen, AH: Ankogel-Hochalmspitzgruppe, Da: Dachsteingruppe, De: Defregger-gruppe, G: Glocknergruppe, GS: Granatspitzgruppe, K: Karnische Alpen, L: Lechtaler Alpen, O: Ötztaler Alpen, R: Rätikon, Ri: Rieserfernergruppe, SK: Salzburger Kalkalpen, S: Samnaun-gruppe, So: Schobergruppe, Si: Silvrettagruppe, Sb: Sonnblickgruppe, St: Stubaier Alpen, V: Venedigergruppe, Vw: Verwallgruppe, Z: Zillertaler Alpen. 1: Innsbruck, 2: Kötschach-Mauthen, 3: Kremsmünster, 4: Linz-Stadt, 5: Mariapfarr, 6: Marienberg/Montemaria, 7: Patscher Kofel, 8: Rauris, 9: Sonnblick, 10: Villacher Alpe, 11: Zugspitze, 12: Davos, 13: Säntis.

A. Fischer et al.

Title Page

Abstract | Introduction

Conclusions | References

Tables | Figures

|◄ | ►|

◄ | ►

Back | Close

Full Screen / Esc

Printer-friendly Version

Interactive Discussion
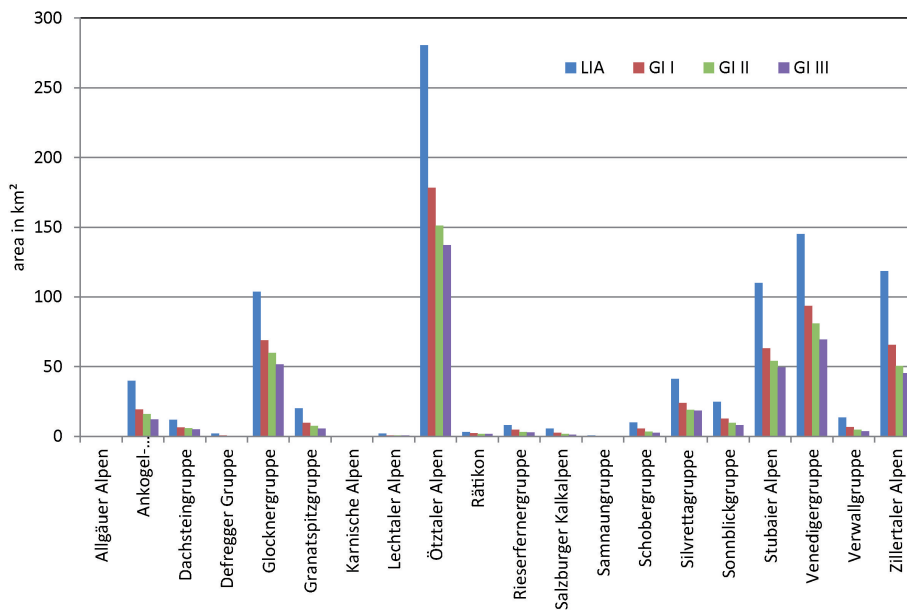
Figure 2. Areas in the specific mountain ranges recorded in the glacier inventories.
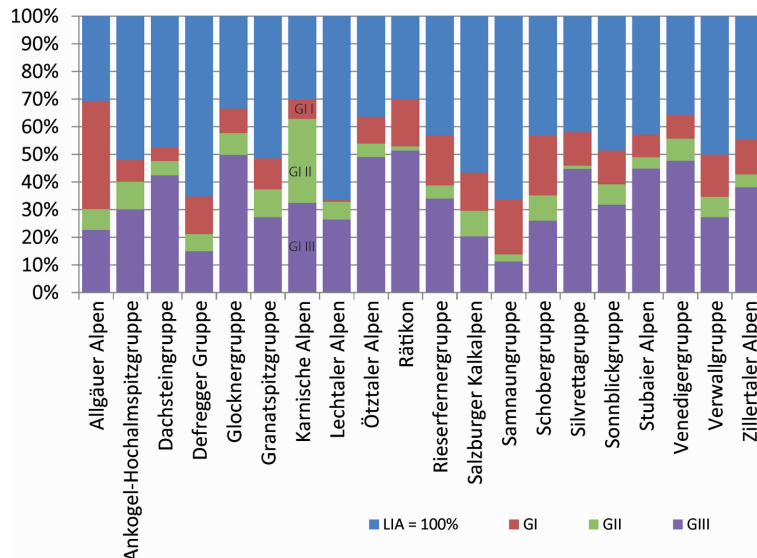
Figure 3. Percentage of LIA glacier area for specific mountain ranges.
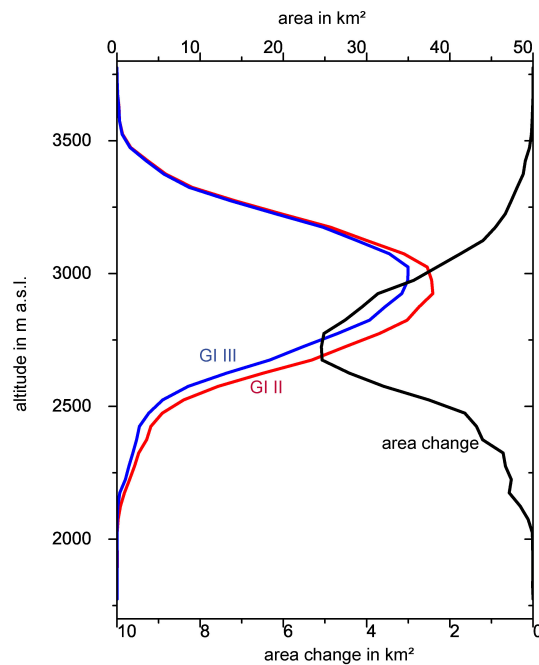
**Figure 4.** Altitudinal distribution of glacier areas and area losses for GI II and GI III by reference to the 1998 DEM.

Title Page

Abstract | Introduction

Conclusions | References

Tables | Figures

|◄ | ►|

◄ | ►

Back | Close

Full Screen / Esc

Printer-friendly Version

Interactive Discussion
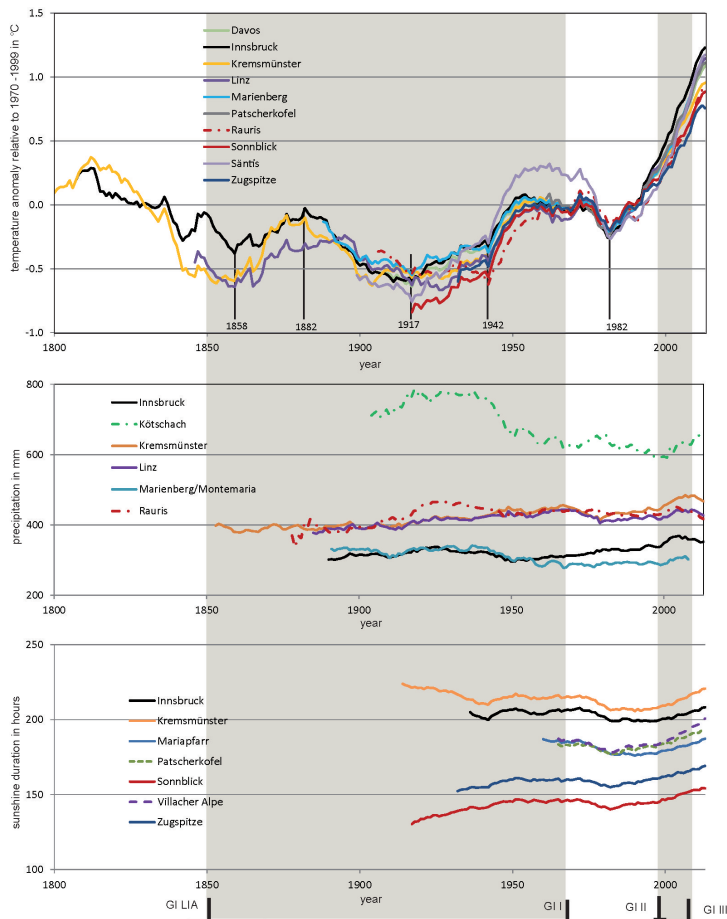
Figure 5. 30 year running means of summer air temperatures (mean June to September), winter precipitation (sum October to April) and summer sunshine duration (sum June to September) for the stations listed in Table 2.